



# Fundamental Investigation of Silicon Anode in Lithium-Ion Cells

*James J. Wu and William R. Bennett  
Glenn Research Center, Cleveland, Ohio*

## NASA STI Program . . . in Profile

Since its founding, NASA has been dedicated to the advancement of aeronautics and space science. The NASA Scientific and Technical Information (STI) program plays a key part in helping NASA maintain this important role.

The NASA STI Program operates under the auspices of the Agency Chief Information Officer. It collects, organizes, provides for archiving, and disseminates NASA's STI. The NASA STI program provides access to the NASA Aeronautics and Space Database and its public interface, the NASA Technical Reports Server, thus providing one of the largest collections of aeronautical and space science STI in the world. Results are published in both non-NASA channels and by NASA in the NASA STI Report Series, which includes the following report types:

- **TECHNICAL PUBLICATION.** Reports of completed research or a major significant phase of research that present the results of NASA programs and include extensive data or theoretical analysis. Includes compilations of significant scientific and technical data and information deemed to be of continuing reference value. NASA counterpart of peer-reviewed formal professional papers but has less stringent limitations on manuscript length and extent of graphic presentations.
- **TECHNICAL MEMORANDUM.** Scientific and technical findings that are preliminary or of specialized interest, e.g., quick release reports, working papers, and bibliographies that contain minimal annotation. Does not contain extensive analysis.
- **CONTRACTOR REPORT.** Scientific and technical findings by NASA-sponsored contractors and grantees.

- **CONFERENCE PUBLICATION.** Collected papers from scientific and technical conferences, symposia, seminars, or other meetings sponsored or cosponsored by NASA.
- **SPECIAL PUBLICATION.** Scientific, technical, or historical information from NASA programs, projects, and missions, often concerned with subjects having substantial public interest.
- **TECHNICAL TRANSLATION.** English-language translations of foreign scientific and technical material pertinent to NASA's mission.

Specialized services also include creating custom thesauri, building customized databases, organizing and publishing research results.

For more information about the NASA STI program, see the following:

- Access the NASA STI program home page at <http://www.sti.nasa.gov>
- E-mail your question to [help@sti.nasa.gov](mailto:help@sti.nasa.gov)
- Fax your question to the NASA STI Information Desk at 443-757-5803
- Phone the NASA STI Information Desk at 443-757-5802
- Write to:  
STI Information Desk  
NASA Center for AeroSpace Information  
7115 Standard Drive  
Hanover, MD 21076-1320



# Fundamental Investigation of Silicon Anode in Lithium-Ion Cells

*James J. Wu and William R. Bennett  
Glenn Research Center, Cleveland, Ohio*

National Aeronautics and  
Space Administration

Glenn Research Center  
Cleveland, Ohio 44135

## Acknowledgments

The authors thank Michelle A. Manzo for her constructive suggestions and inputs, and significant effort in revisions. The authors thank Eunice Wong for sharing her report for SEM analysis results. The authors also thank all the anode team members of the Electrochemistry Branch for their help and discussion. This work was performed in support NASA's High Efficiency Space Power Systems (HESPS) Project, which is developing advanced lithium-ion cells for future NASA exploration missions under the Enabling Technology Development and Demonstration (ETDD) Program. This work, which began under the Exploration Technology Development Program (ETDP) Energy Storage Project, combines the efforts of industrial partners and contractors to develop aerospace cell designs with enhanced specific energy and safety characteristics.

This report is a formal draft or working paper, intended to solicit comments and ideas from a technical peer group.

*Level of Review:* This material has been technically reviewed by technical management.

Available from

NASA Center for Aerospace Information  
7115 Standard Drive  
Hanover, MD 21076-1320

National Technical Information Service  
5301 Shawnee Road  
Alexandria, VA 22312

Available electronically at <http://www.sti.nasa.gov>

# Fundamental Investigation of Silicon Anode in Lithium-Ion Cells

James J. Wu and William R. Bennett  
National Aeronautics and Space Administration  
Glenn Research Center  
Cleveland, Ohio 44135

## Abstract

Silicon is a promising and attractive anode material to replace graphite for high capacity lithium ion cells since its theoretical capacity is ~10 times of graphite and it is an abundant element on Earth. However, there are challenges associated with using silicon as Li-ion anode due to the significant first cycle irreversible capacity loss and subsequent rapid capacity fade during cycling. Understanding solid electrolyte interphase (SEI) formation along with the lithium ion insertion/de-insertion kinetics in silicon anodes will provide greater insight into overcoming these issues, thereby lead to better cycle performance. In this paper, cyclic voltammetry and electrochemical impedance spectroscopy are used to build a fundamental understanding of silicon anodes. The results show that it is difficult to form the SEI film on the surface of a Si anode during the first cycle; the lithium ion insertion and de-insertion kinetics for Si are sluggish, and the cell internal resistance changes with the state of lithiation after electrochemical cycling. These results are compared with those for extensively studied graphite anodes. The understanding gained from this study will help to design better Si anodes, and the combination of cyclic voltammetry with impedance spectroscopy provides a useful tool to evaluate the effectiveness of the design modifications on the Si anode performance.

## Introduction

NASA is developing ultra-high energy Li-ion cells and batteries for future exploration missions. These cells will utilize advanced anode materials to replace graphite. Silicon is a promising candidate since its theoretical capacity is ~10 times that of graphite (Refs. 1 and 2), and it is an abundant element on Earth. However, the use of Si anodes in Li-ion batteries is challenging due to its significantly lower conductivity and much higher (~400 percent) volume expansion during lithiation and de-lithiation that occur during the cycling processes (Ref. 3). Much research has been conducted on Si anodes aimed at addressing these limitations. Approaches include the addition of carbon fibers or carbon black for improvement of Si conductivity (Refs. 4 and 5), the development of Si/C composite electrodes (Ref. 6) and the use of nano Si wires for reduction of expansion (Refs. 7 to 9). Much progress has been made on these fields.

This study focuses on developing an understanding of the solid electrolyte interphase (SEI) and Li-ion insertion/de-insertion kinetics in cells with silicon anodes. The SEI is a passivating film that is formed on the anode surface by electrolyte decomposition in a lithium ion battery. This film protects the electrolyte solution from further decomposition, and also affects the safety, power capacity, shelf life, cycle life and performance of a lithium-ion battery (Refs. 10 to 12). However, the SEI film also limits the capacity and dynamic response of Li-ion batteries by limiting lithium ion transport, and the resistance across the film also restricts the current flow. For optimal performance, the SEI should be highly permeable to lithium ions to minimize the concentration polarization and must be an electronic resistor to prevent SEI thickening that leads to high internal resistance, self-discharge and low faradaic efficiency. The SEI should also be highly ion-conductive to reduce overvoltage, and have uniform chemical composition and morphology to ensure homogeneous current distribution. Gaining a fundamental understanding of the phenomena that control the formation of the SEI is essential to the ability to design efficient Si anodes. The interfacial phenomena and SEI formation in lithium-based cells have been analyzed by impedance spectroscopy (Refs. 9, 13 to 15); lithium insertion/de-insertion kinetics in a single

silicon electrode particle was analyzed by cyclic voltammetry, and a model for a single Si particle that accounts for the volume change during insertion/de-insertion process was developed (Ref. 16). Numerous new techniques such as X-ray Photoelectron Spectroscopy (XPS), X-ray Diffraction (XRD), Surface-Enhanced Raman Spectroscopy (SERS), Scanning Electron Microscopy (SEM)/Energy-Dispersive X-ray Spectroscopy (EDS), Fourier Transform Infrared Spectroscopy (FT-IR), Nuclear Magnetic Resonance (NMR), EPR, Calorimetry, DSC, TGA, Quartz Crystal Microbalance (QCMB), Atomic-Force microscopy (AFM) and in-situ Neutron Radiography have been recently adapted to study the electrode surface and the chemical and physical properties of the SEI (Ref. 17).

In this article, cyclic voltammetry and electrochemical impedance spectroscopy are used for the investigation of anode/electrolyte interface, solid electrolyte interphase (SEI) formation and lithium ion transfer kinetics during the electrochemical lithiation and de-lithiation processes for Si and graphite anodes. Cyclic voltammetry not only provides the insights into the SEI formation and lithium ion insertion/de-insertion kinetics, but also provides useful information related to the electrochemical stabilities of the electrolyte and electrodes, the presence of any side reactions and the window (range) of potentials used for electrochemical cycling. Cyclic voltammetry is also a useful tool for studying electrode reversibility of charge and discharge and provides a quick prediction of cycling performance. Electrochemical impedance spectroscopy is a non-destructive technique that is useful for investigating the electrode/electrolyte interface and can elucidate SEI formation mechanism and elements such as the resistance and capacitance of the SEI film. The experimental results obtained with Si anodes are compared with similar assessments of well-established graphite anodes. These studies help develop an understanding of the Si anode and provide insight into how to address irreversible capacity loss and capacity fade in Si anodes.

## **Experimental**

### **Coin Cell Construction**

#### **Anode Materials, Separator and Electrolyte**

The Si anode used in this investigation was developed by Lockheed Martin under a NASA Research Announcement contract that was part of the Enabling Technology Development and Demonstration (ETDD) program, High Efficiency Space Power System (HESPS) battery development effort. The Si anode consisted of silicon, polyimide and carbon. The graphite anode for the comparison study was provided by Saft America. The graphite electrode was originally coated on both sides, and one side coating was removed for this study. The graphite anode was composed of Mitsubishi Power Graphite (MPG) 111, and styrene butadiene rubber (SBR) and carboxy methyl cellulose (CMC) as binder. The separator was 20  $\mu\text{m}$  polyethylene (PE) from Tonen. The electrolyte was 1M  $\text{LiPF}_6$  in EC:DEC:DMC (1:1:1 v/v).

#### **Coin Cell Fabrication**

Coin cell fabrication 2325 type coin cells were fabricated for the electrochemical characterization tests. A thin disk (with diameter of 0.5 in.) of Si anode or graphite anode was used as working electrode, and a disk (with a diameter of 0.625 in.) of Li metal was used as the counter electrode. The coin cell was constructed in the following sequence and configuration: positive can, anode disk, separator, Li metal, spacer, spring, and then negative cover, as shown in Figure 1. A quantity of 60  $\mu\text{l}$  of electrolyte was added in two steps: the 1<sup>st</sup> 30  $\mu\text{l}$  was added to anode electrode, the separator was stacked on the anode and then the remaining 30  $\mu\text{l}$  was added to the separator. Subsequently, the Li metal counter electrode was put on top of the separator, followed by the spacer and spring, and finally the negative cell cover was added and the coin cell was closed. The assembly process for the coin cells was conducted in a glove box filled with Argon. A total of 13 coin cells, 8 with silicon anodes and 5 with carbon anodes, were built for the cyclic voltammetry scan rate tests and impedance measurements.

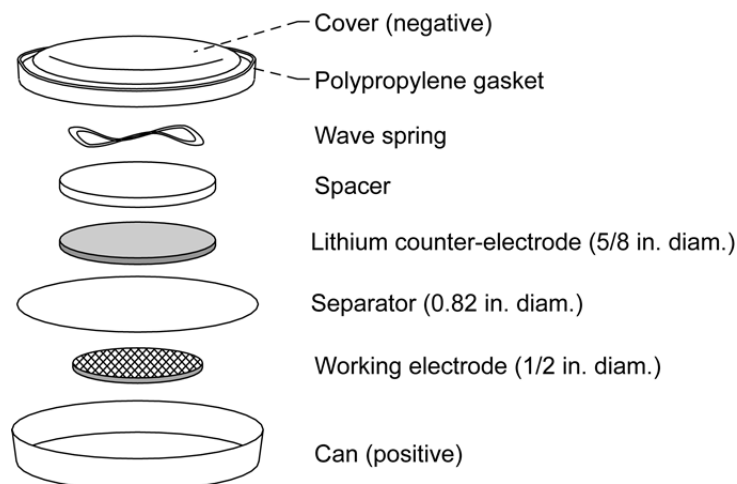


Figure 1.—Schematic of coin cell components and construction.

## Electrochemical Measurements

Cyclic Voltammetry (CV) measurements were conducted with an Arbin Instrument BT-2000. For the coin cells with Si anodes, the potential was initially scanned from open circuit voltage (OCV) to 0.05 V and then back to 1 V for the first cycle, and the scan voltage is set between 1 and 0.05 V for the subsequent cycles. Similarly, for the coin cells with graphite anodes, the potential was initially scanned from OCV to 0.01 V, and then back to 1 V for the first cycle, and for the subsequent cycles, the scan voltage was set between 1 and 0.01 V. Scan rates of 1, 0.5, 0.25, and 0.125 mV/sec were used in the CV study. A new cell was used for each scan rate test.

Electrochemical Impedance Spectroscopy (EIS) measurements were conducted on a SI 1287 Electrochemical Interface coupling with SI 1260 Impedance/Gain-phase Analyzer. The impedance was measured before and after the cyclic voltammetry tests. The typical frequency range was between 500 kHz to 100 mHz and the applied AC voltage was 10 mV. The analysis of the resultant Nyquist plots was conducted with ZPlot/Zview software (Solartron Analytical). The potentials in this paper are referenced to  $\text{Li/Li}^+$ .

## Results and Discussions

### SEM Analysis of Anode Electrodes

The Si anode and the graphite anode used for these investigations were characterized by SEM. Selected pictures are shown in Figure 2. The Si anode has a rough and compacted surface with some cracks and agglomerates of Si and C particles, as shown in Figure 2(a).

The sizes of Si particles are too small to be determined accurately, but most of the particle sizes are  $<200$  nm, as shown in the high magnification photo in Figure 2(b). The graphite anode shown in Figure 2(c) has a more even and uniform surface than the Si. The typical graphite particle sizes are in the range of 10 to 20  $\mu\text{m}$ , as seen in Figure 2(d). The SEM pictures indicate that the graphite anode was probably calendared while the Si anode was not. The quality and uniformity of the Si anode are not as good as for the graphite anode.

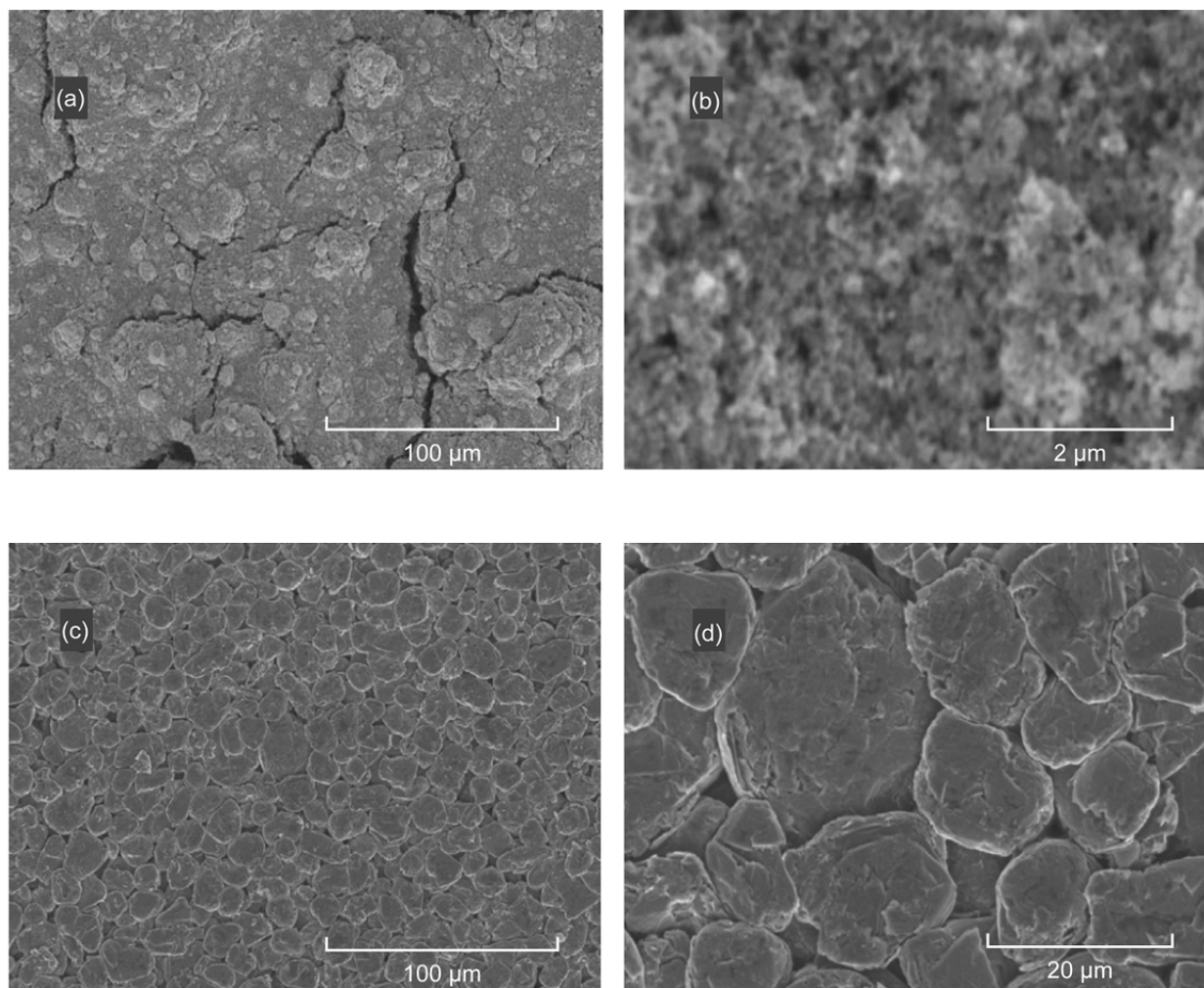


Figure 2.—SEM of the Si anode (a) and (b), and the graphite anode (c) and (d). Magnification: (a) 500 $\times$ ; (b) 20,000 $\times$ ; (c) 500 $\times$ ; (d) 2,000 $\times$ .

### Cyclic Voltammetry Study

**Solid Electrolyte Interphase (SEI) Formation** The SEI is a passivating film that is formed on the anode surface by salt-mediated electrolyte decomposition. This film protects the electrolyte solution from further decomposition. Cyclic voltammetry was used to study the electrolyte decomposition and SEI formation. As the potential scans cathodically from open circuit voltage (OCV, typical  $\sim 3$  V) to 0.05 V for the Si anode at the first cycle, the SEI film starts being formed (at  $\sim 0.5$  to 0.8 V) due to the electrolyte decomposition. Ideally, the SEI blocks electrolyte solvents and only the lithium ion can pass through the SEI film and insert into Si anode (at  $\sim 0.2$  V). This electrochemical lithiation process is reflected by the cathodic current. The potential is cathodically scanned to 0.05 V, and the potential of 0.05 V is used to avoid the most severe volume expansion region of Si which occurs at  $<0.05$  V. As the potential is scanned back to 1 V, the inserted lithium ions are de-inserted from the Si anode. This electrochemical de-insertion process is reflected by the anodic current. As shown in Figure 3(a), the SEI film for Si anode does not seem to be completely formed in the first cycle since further electrolyte decomposition is observed and the cathodic current continues to increase with cycling. The much lower anodic current versus the cathodic current in the first cycle indicates less lithium is de-lithiated, and the charge consumed by electrolyte decomposition in the first cycle for Si anode results in significant irreversible capacity loss.



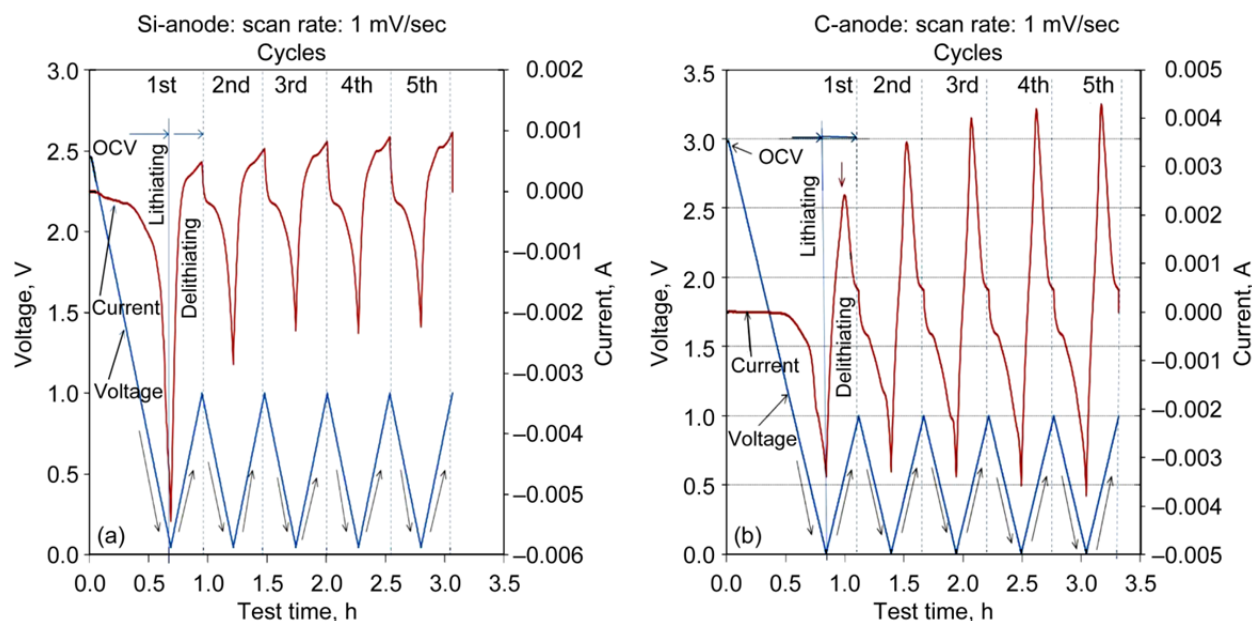


Figure 3.—The profile of current, voltage versus time of the initial 5 cycles in the cyclic voltammetry measurement. (a) Si anode; (b) graphite anode.

As the electrochemical cycles increase, the SEI film appears to be slowly formed in the subsequent scans as the cathodic current and anodic current tend to stabilize, as shown in Figure 3(a). The result shows that the SEI film is difficult to form for the cells with Si anodes.

The profile of potential and current versus time for the graphite anode is different from the Si anode, as shown in Figure 3(b). The potential is cathodically scanned to 0.01 V. The potential of 0.01 V is used to maximize the lithium ion insertion into graphite but to avoid the reduction of the lithium ion to form lithium metal on graphite during the electrochemical lithiation process. The SEI film is formed relatively easily versus Si anode in the first cycle since the electrolyte decomposition is stopped and the cathodic current does not further increase. The slightly higher cathodic current than the corresponding anodic current at the 1<sup>st</sup> cycle indicates that there is small irreversible capacity loss at the 1<sup>st</sup> cycle. Starting from the 3<sup>rd</sup> cycle, the formed SEI layer is stabilized, as reflected from the stabilized cathodic current from the lithium insertion process and anodic current from de-insertion process.

The most common expression for the cyclic voltammetry is the plot of the generating current (i) versus the corresponding applied potential. Figures 4(a) and 5(a) are the corresponding profiles of Figures 3(a) and (b), respectively. The difference between the cyclic voltammetry response for the Si anodes and graphite anodes is clearly seen. The major difference is in the first cycle. There are several more distinct differences in the cyclic voltammograms for the Si and graphite anodes; the Si anode has poorer reversibility than the graphite anode; the de-lithiation peak ( $\sim 0.6$  V) for the Si anode is more positive than the de-lithiation peak ( $\sim 0.3$  V) for the graphite anode at the same scan rate; and the de-lithiation peak for Si anode is broader than the de-lithiation peak for graphite anode, implying a slow kinetic process of lithium ion insertion/de-insertion in the Si anode.

## Lithium Ion Insertion/De-insertion Kinetics

Cyclic voltammetry was also used to study lithium ion insertion/de-insertion kinetics for Si anodes. Figures 4(a) to (d) are the cyclic voltammograms of Si anodes at various scan rates of 1, 0.5, 0.25, and 0.125 mV/sec, respectively. At the scan rate of 1 mV/sec, not many lithium ions are inserted into the Si anode, as evidenced by the lack of noticeable anodic current from the de-lithiation process. As the scan rate decreases, the cathodic current decreases, and the corresponding anodic current increases from the first cycle, which indicates that more lithium ions are inserted into the Si anode, thus more lithium ions can be de-inserted from the Si anode. It also shows that the anodic peak (from de-lithiation process) becomes narrower as the scan rate decreases. All the above observations indicate that the lithium ion insertion and de-insertion to and from Si anodes is a sluggish process. This agrees with findings from the cyclic voltammetry study of single Si particle (Ref. 16). The broader peak width seen for the de-insertion for the Si anode also implies that the insertion/de-insertion process is slow, which implies that the high rate charge/discharge cycling may be impacted.

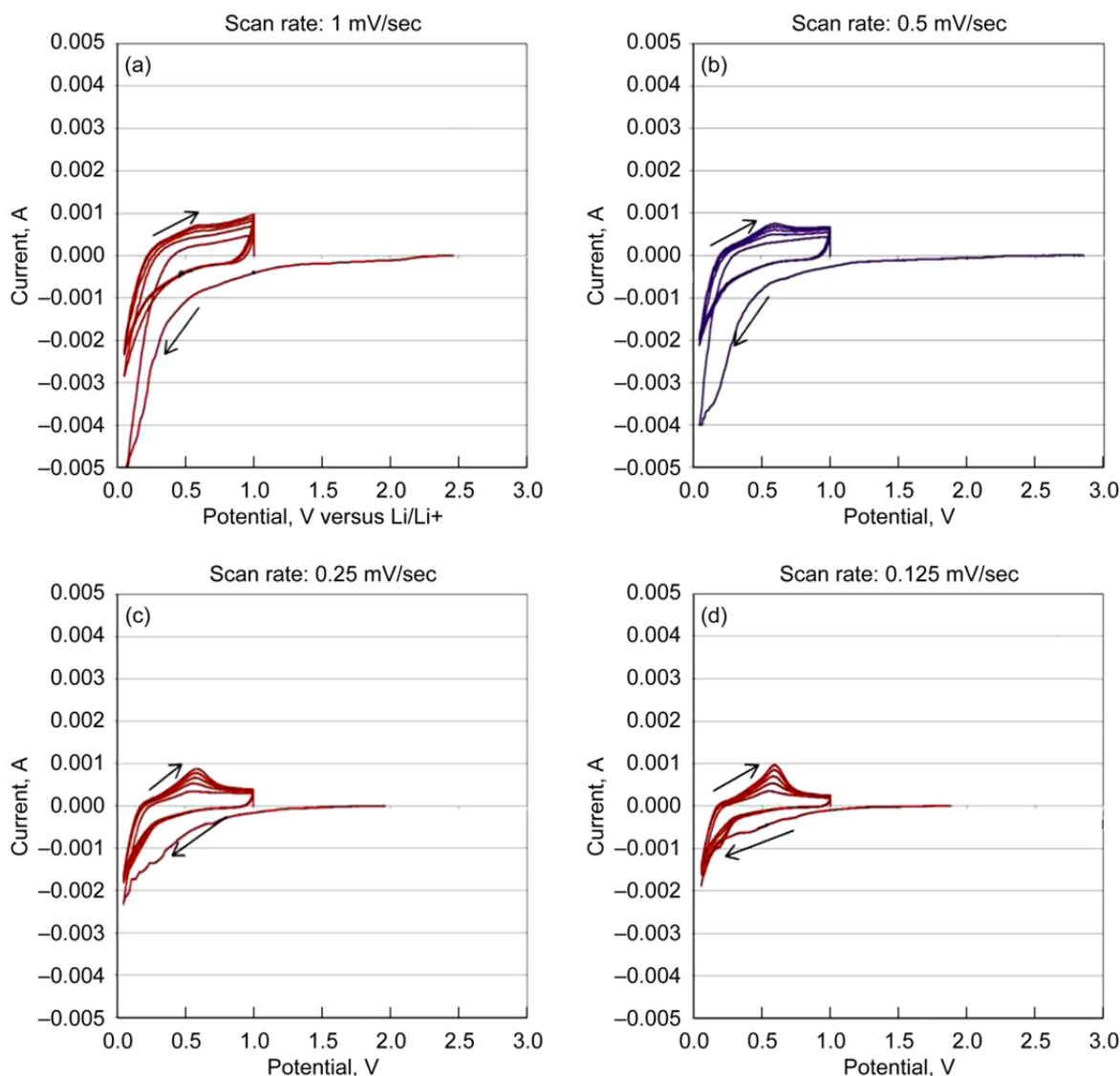


Figure 4.—Cyclic voltammograms (the initial 5 cycles) of Si anode in Li/Si coin half-cell with various scan rates: (a) 1 mV/sec; (b) 0.5 mV/sec; (c) 0.25 mV/sec; (d) 0.125 mV/sec.

The cyclic voltammograms of the graphite anodes at various scan rates, shown in Figures 5(a) to (d), are quite different from those for the Si anode. The de-lithiation peak for graphite anode is much narrower than for the Si anode. The de-lithiation peak height for graphite anodes does not change as greatly as seen for the Si anode. However, the de-lithiation peak width for graphite anode decreases as the scan rate decreases. These results indicate that the lithium ion insertion/de-insertion process in graphite anode is faster than the Si anode.

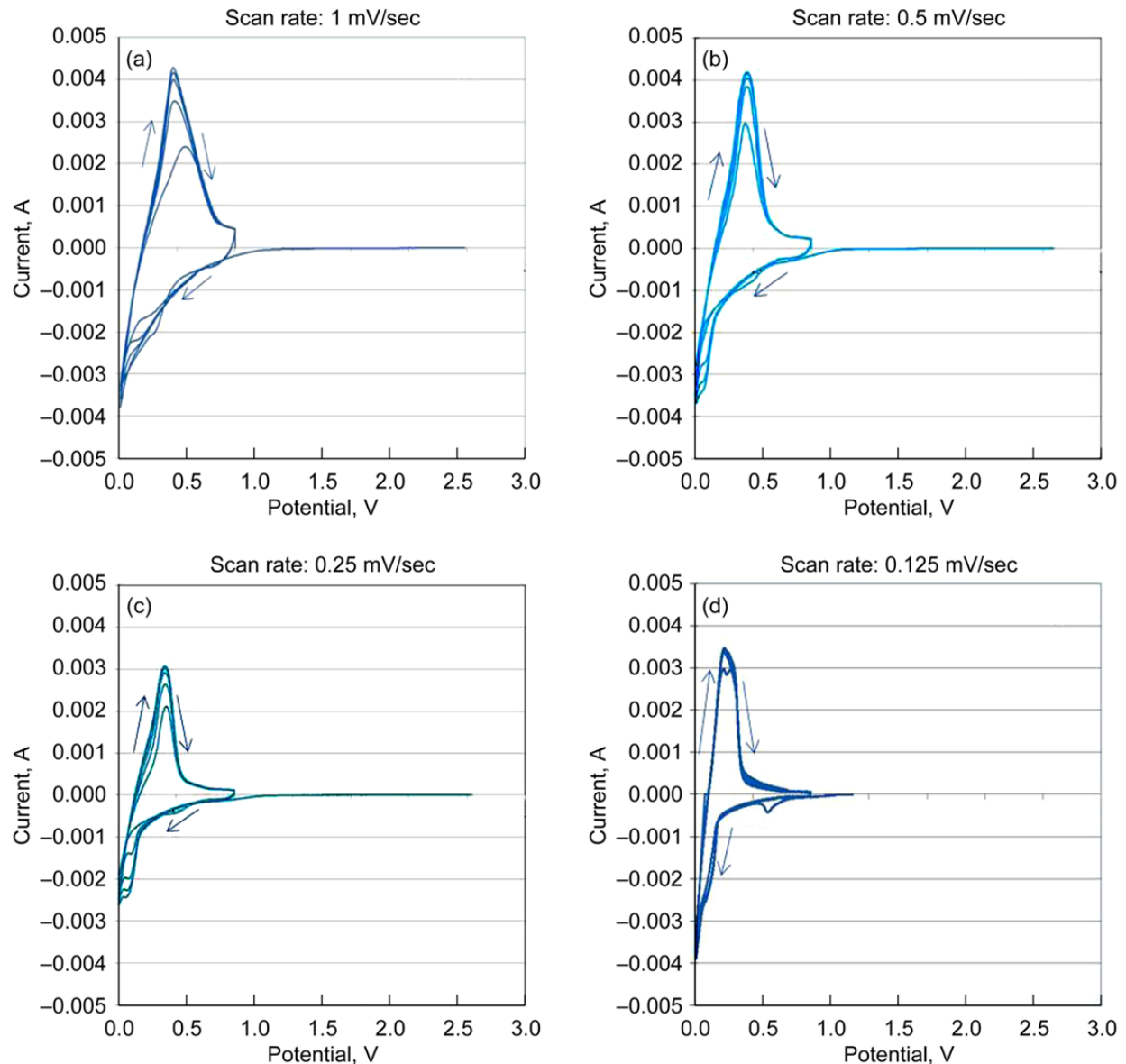


Figure 5.—Cyclic voltammograms (the initial 5 cycles) of graphite anode in Li/C coin half cell with various scan rates. (a) 1 mV/sec; (b) 0.5 mV/sec; (c) 0.25 mV/sec; (d) 0.125 mV/sec.

## Electrochemical Impedance Spectroscopy Study

Electrochemical impedance spectroscopy is a non-destructive and useful tool to study the electrochemical behavior of electrode materials and their interfacial properties, such as resistance and capacitance of SEI film formation. Figure 6(a) shows the typical impedance spectra for cells with Si anodes and graphite anodes which were built just before electrochemical cycling. The cells with Si anode and the cells with graphite anode have similar features, i.e., a depressed semi-circle and a tail, implying mixed kinetics and diffusion processes. The equivalent circuit of the cells with Si anode and the cells with graphite anode are the same, as shown in the top of Figure 6(b). The fitted data, which represents the average of at least three cells, shows the corresponding components in the bottom portion of Figure 6(b). The results show that the cell internal resistance  $R_{int}$ , which is the sum of electronic resistance from the electrode material, separator, contact between active materials with the current collector and the ionic resistance of the electrolyte, is higher for the cell with Si anode than for the cell with graphite anode. This is reasonable as the Si itself has lower conductivity than the graphite, and the percentage of active material in the Si anode is lower than in the graphite anode. Since the Si has much a smaller particle size (mostly <200 nm) than the graphite particle (mostly 10 to 20  $\mu\text{m}$ ), the Si anode has a smaller charge transfer resistance and a higher capacitance than the graphite anode initially.

In combination with the cyclic voltammetry measurement, the impedance was measured after the potential scans to the desired states, such as at 1.0 V (de-lithiated state), and at 0.05 V for Si anode (lithiated state) following the initial 5<sup>th</sup> cycle for the cells with Si anode. Figure 7(a) shows that the impedance spectra before cycling, after scanning to 1.0 V and after scanning to 0.05 V for the cells with Si anodes. The charge transfer resistance of the cell, after electrochemical cycling, is lower than before cycling. This is explained the fact that the surface of the Si electrode is initially covered with a non-conducting native layer consisting of silicon oxide and silanol (Ref. 19). After electrochemical cycling, the native layer is broken down, which is possibly caused by the  $\text{Li}^+$  diffusion through the native surface layer, and thus the charge transfer resistance becomes lower. However, the internal resistance,  $R_{int}$ , of the cells after electrochemical cycling is higher than before cycling, as shown in Figure 7(b), and

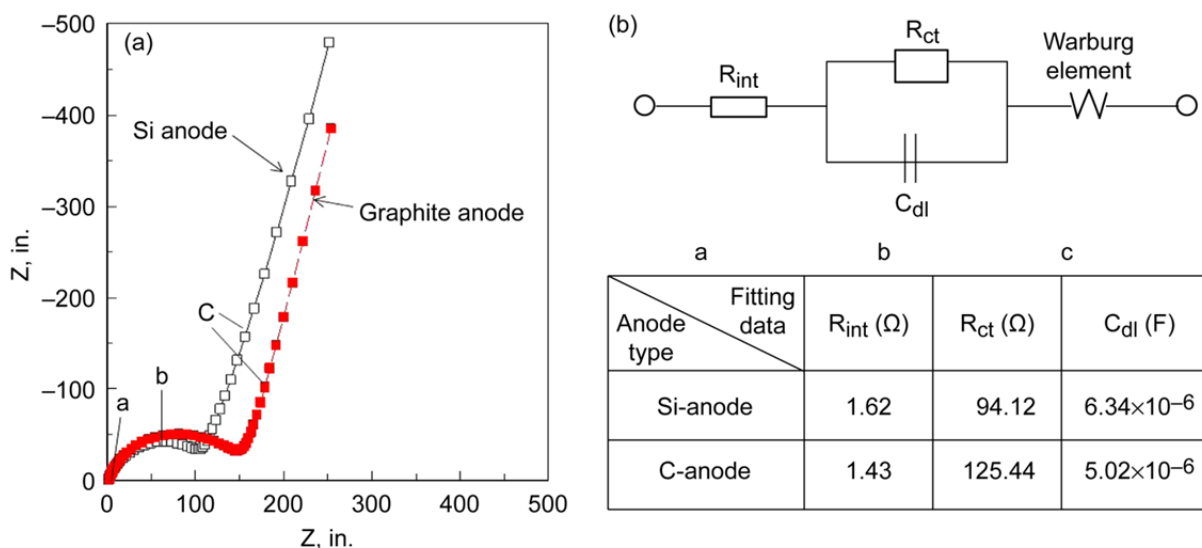


Figure 6.—Impedance spectra of comparing cells with Si anode and graphite anodes before the electrochemical cycling (a): typical Nyquist plot; (b) the equivalent circuit used to fit impedance data,  $R_{int}$  is the cell internal resistance,  $R_{ct}$  is the charge transfer resistance,  $C_{dl}$  is the double layer pseudocapacity, and Warburg element is the solid state diffusion element.

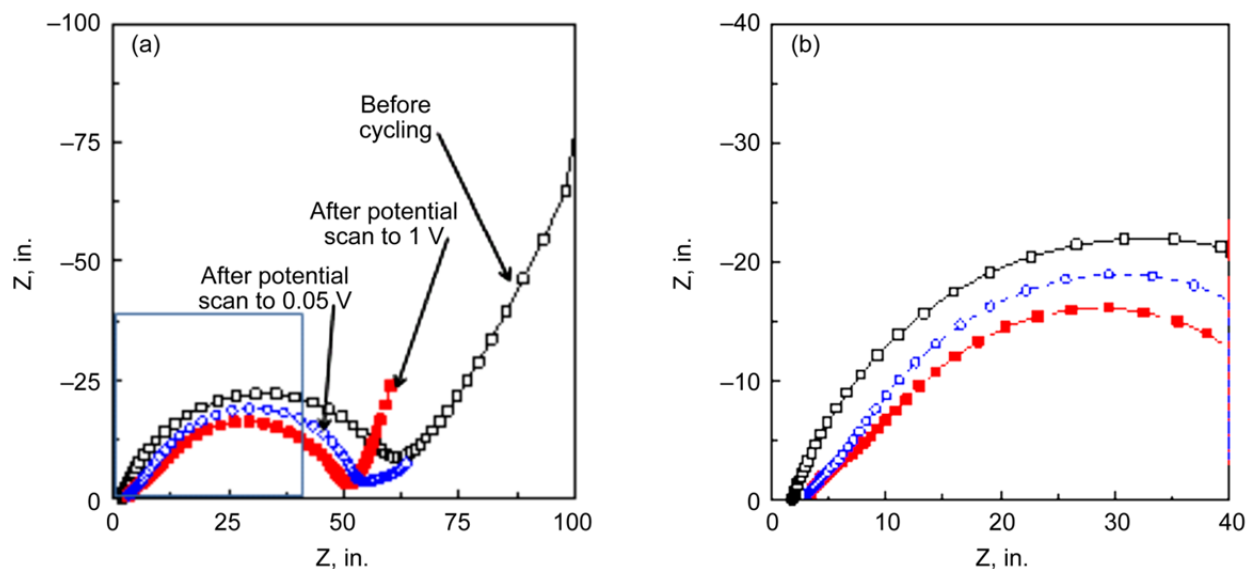


Figure 7.—Impedance spectra of the cell with Si anode (a) Nyquist plot; (b) the amplification of the square part in (a).

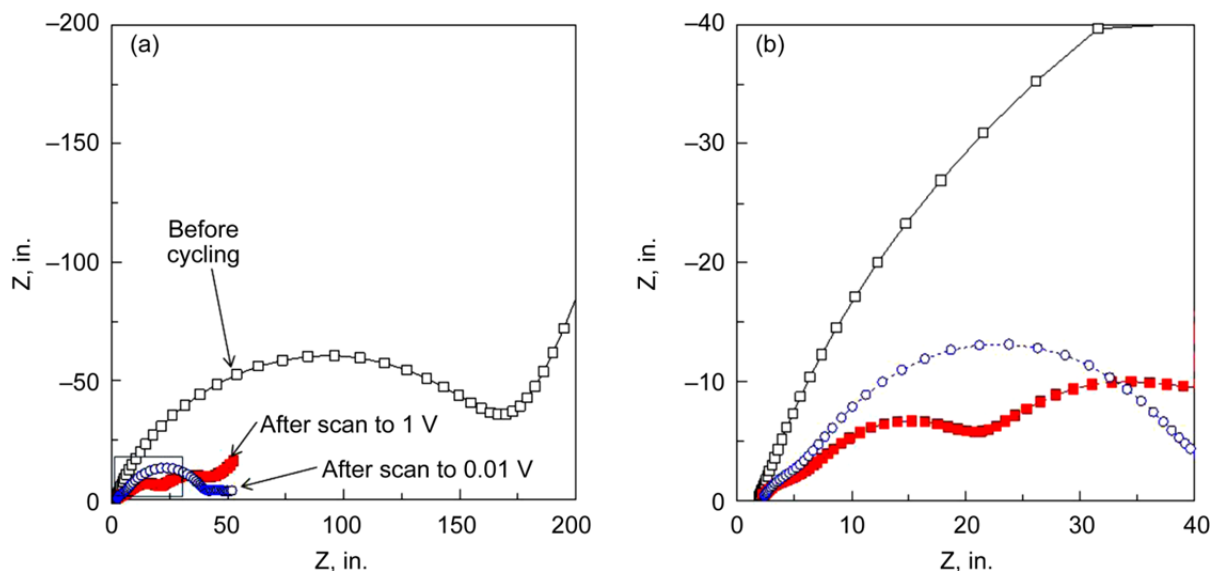


Figure 8.—Impedance spectra of the cell with graphite anode (a) Nyquist plot; (b) the amplification of the square part in (a).

this resistance increase is believed to the growth of SEI layer on the Si electrode. There is a very small, non-obvious depressed semicircle at the high frequency end, which is indicative of the formation of the surface SEI film. In addition, the fitted results show that the cell internal resistance at 1 V (de-lithiated,  $2.94 \Omega$ ) is slightly higher than at 0.05 V (lithiated,  $2.83 \Omega$ ), and both values are much higher than the internal resistance before cycling ( $1.74 \Omega$ ). This is probably because the volume contraction of the de-lithiated state (after volume expansion at lithiated state) causes the Si particle shape changes and thus results in loss of Si-Si particle contact and causes higher internal resistance.

Similar procedures were used to analyze the cells with graphite anodes. Figure 8(a) shows the impedance spectra before cycling, after scanning to 1.0 V (de-lithiated state) and after scanning to 0.01 V (lithiated state) after 5<sup>th</sup> cycle of cyclic voltammetry measurement. The charge transfer resistance of the cells is significantly reduced after electrochemical cycling. This is due to  $\text{Li}^+$  quick diffusion into the graphite anode. There are two semicircles after scanning to 0.01 V (lithiated state) as in the cells with the

Si anode. The small semicircle at the high frequency end corresponds to SEI film formation. It is interesting to find that there are three semicircles after scanning to 1.0 V (de-lithiated state), as shown in Figures 8(a) and (b), indicating multilayer films formed on the graphite anode, which is different from the cells with Si anodes.

The internal resistance of the cells with graphite anode is higher after cycling than before cycling, which is caused by the growth of the SEI. The fitted results show that the cell internal resistance at 1 V (de-lithiated, 1.96  $\Omega$ ) is only slightly higher than at 0.01 V (lithiated, 1.91  $\Omega$ ), slightly higher than the internal resistance before cycling (1.40  $\Omega$ ). This is because the volume contraction of the de-lithiated state (after volume expansion at lithiated state) for graphite anode is small, thus the resistance change after lithiation and de-lithiation process is small.

## Conclusion

Cyclic voltammetry measurements show that the SEI formation on Si anode is difficult, the 1<sup>st</sup> cycle irreversible capacity loss is significant and the reversibility is poor for the initial cycles for a Si anode. However, SEI formation on graphite anodes is easier, the 1<sup>st</sup> cycle capacity loss is small and the reversibility is good during the initial few cycles. This is probably related to the SEI formation properties. The cyclic voltammetry measurements at various potential scan rates also indicate that the kinetics of the lithium ion insertion and de-insertion processes for the Si anode are sluggish, while the kinetics for the graphite anode are fast. Impedance spectroscopy measurements further demonstrate that the cell with the Si anode has a higher initial resistance than the cell with the graphite anode, and the SEI formation results in an increase in the cell internal resistance for both the Si and graphite anodes. The SEI formed at the Si anode is more resistive than the SEI formed at the graphite anode. There is also a change in the cell internal resistance between the lithiated state and de-lithiated state of the Si anode, but this change is small for the graphite anode. The internal resistance change of the graphite anode is around half of that of Si anode. In addition, the charge transfer resistance after electrochemical cycling for the cell with the Si anode is appropriately twice as high as that for the cell with the graphite anode, implying slow lithium kinetics in the Si anode. The difficult SEI formation, higher initial cell internal resistance, and higher SEI resistance, as well as the greater resistance change during the lithiation and de-lithiation processes may explain the higher irreversible capacity loss and capacity fade for the Si anode.

Future work will evaluate the effects of surface reactive additives to the electrolyte to promote fast SEI formation and to stabilize the SEI on the Si anode. Efforts to optimize the conductive matrix of the Si anode to lower the volume changes could help to overcome the 1<sup>st</sup> cycle irreversibility and capacity fade. The combination of cyclic voltammetry with impedance spectroscopy is useful to evaluate the effectiveness of the suggested modifications on the Si anode performance.

## References

1. Wen, C.J.; Huggins, R.A. *J. Solid State Chem.* 1981, 37, 271.
2. Besenhard, J.O.; Yang, J.; Winter, M. *J. Power Sources* 1997, 68, 87.
3. Boukamp, B.A.; Lesh, G.C.; Huggins, R.A. *J. Electrochem. Soc.* 1981, 128, 725-729.
4. Xiao, J.; Xu, W.; Wang, D.; Choi, D.W.; Wang, W.; Li, X.L.; Graff, G.L.; Liu, J.; Zhang, J.G. *J. Electrochem. Soc.* 2010, 157, A1047.
5. Wolf, H.; Pajkic, Gerdes, T.; Willert-Porada, M. *J. Power Sources* 2009, 190, 157.
6. Magasinski, A.; Dixon, P.; Hertzberg, B.; Kvit, A.; Ayala, J.; Yushin, G. *Nature Mater.* 2010, 9, 353.
7. Li, H.; Huang, X.; Chen, L.; Wu, Z.; Liang, Y. *Electrochem. Solid-State Lett.* 1999, 2, 547-549.
8. Graetz, J.; Ahn, C.C.; Yazami, R.; Fultz, B. *Electrochem. Solid State-Lett.* 2003, 6, A194-A197.
9. Riccardo R.; Seung, S.H.; Candace, K.C.; Robert, A.H.; Yi, C. *J. Phys. Chem. C* 2009, 113, 11390.
10. Peled E., in *Lithium Batteries*, ed. by Gabano J.P., Academic, 1983, p 43.
11. Funabiki A.; Inaba M.; Abe T. and Ogumi Z. *J. Electrochem. Soc.* 1999, 146, 2443-2448.
12. Peled E.; Golodnitsky D. and Ardel G. *J. Electrochem. Soc.* 1997, 144, L208.

13. Baldwin R.S. and Bennett, W.R. in NASA/TM-2007-214946.
14. Lee, Y.M.; Lee, J.Y.; Shim, H.T.; Lee, J.K. and Park, J.K. *J. Electrochem. Soc.* 2007, 154, A515-A519.
15. Chen, W.Y.; Ou, Z.W.; Tang, H.T.; Wang H. and Yang, Y. *J. Electrochimica Acta* 2008, 53, 4414-4419.
16. Chandrasekaran, R.; Magasinski, A.; Yushin, G. and Fuller, T.F. *J. Electrochem. Soc.* 2010, 157, A1139-A1151.
17. Peled E. and Golodnitsky D., in *Lithium-Ion Batteries Solid-Electrolyte Interphase* ed. By Balbuena P.B. and Wang Y.X. Imperial College Press, 2004, p 2.
18. Wong, E. *Internal Analytical Report*.
19. Yoshio, M.; Wang H.; Fukuda, K.; Umeno, T.; Dimov, N.; and Ogumi, Z. *J. Electrochem. Soc.* 2002, 149, A1598.
20. Mercer C. et al., “Energy Storage Technology Development for Space Exploration,” NASA/TM—2011-216964.

REPORT DOCUMENTATION PAGE				Form Approved OMB No. 0704-0188	
<p>The public reporting burden for this collection of information is estimated to average 1 hour per response, including the time for reviewing instructions, searching existing data sources, gathering and maintaining the data needed, and completing and reviewing the collection of information. Send comments regarding this burden estimate or any other aspect of this collection of information, including suggestions for reducing this burden, to Department of Defense, Washington Headquarters Services, Directorate for Information Operations and Reports (0704-0188), 1215 Jefferson Davis Highway, Suite 1204, Arlington, VA 22202-4302. Respondents should be aware that notwithstanding any other provision of law, no person shall be subject to any penalty for failing to comply with a collection of information if it does not display a currently valid OMB control number.</p> <p>PLEASE DO NOT RETURN YOUR FORM TO THE ABOVE ADDRESS.</p>					
1. REPORT DATE (DD-MM-YYYY) 01-10-2012		2. REPORT TYPE Technical Memorandum		3. DATES COVERED (From - To)	
4. TITLE AND SUBTITLE Fundamental Investigation of Silicon Anode in Lithium-Ion Cells				5a. CONTRACT NUMBER	
				5b. GRANT NUMBER	
				5c. PROGRAM ELEMENT NUMBER	
6. AUTHOR(S) Wu, James, J.; Bennett, William, R.				5d. PROJECT NUMBER	
				5e. TASK NUMBER	
				5f. WORK UNIT NUMBER WBS 152964.04.01.01.01.03	
7. PERFORMING ORGANIZATION NAME(S) AND ADDRESS(ES) National Aeronautics and Space Administration John H. Glenn Research Center at Lewis Field Cleveland, Ohio 44135-3191				8. PERFORMING ORGANIZATION REPORT NUMBER E-18484	
9. SPONSORING/MONITORING AGENCY NAME(S) AND ADDRESS(ES) National Aeronautics and Space Administration Washington, DC 20546-0001				10. SPONSORING/MONITOR'S ACRONYM(S) NASA	
				11. SPONSORING/MONITORING REPORT NUMBER NASA/TM-2012-217739	
12. DISTRIBUTION/AVAILABILITY STATEMENT Unclassified-Unlimited Subject Categories: 15, 20, and 44 Available electronically at <a href="http://www.sti.nasa.gov">http://www.sti.nasa.gov</a> This publication is available from the NASA Center for AeroSpace Information, 443-757-5802					
13. SUPPLEMENTARY NOTES					
14. ABSTRACT Silicon is a promising and attractive anode material to replace graphite for high capacity lithium ion cells since its theoretical capacity is ~10 times of graphite and it is an abundant element on Earth. However, there are challenges associated with using silicon as Li-ion anode due to the significant first cycle irreversible capacity loss and subsequent rapid capacity fade during cycling. Understanding solid electrolyte interphase (SEI) formation along with the lithium ion insertion/de-insertion kinetics in silicon anodes will provide greater insight into overcoming these issues, thereby lead to better cycle performance. In this paper, cyclic voltammetry and electrochemical impedance spectroscopy are used to build a fundamental understanding of silicon anodes. The results show that it is difficult to form the SEI film on the surface of a Si anode during the first cycle; the lithium ion insertion and de-insertion kinetics for Si are sluggish, and the cell internal resistance changes with the state of lithiation after electrochemical cycling. These results are compared with those for extensively studied graphite anodes. The understanding gained from this study will help to design better Si anodes, and the combination of cyclic voltammetry with impedance spectroscopy provides a useful tool to evaluate the effectiveness of the design modifications on the Si anode performance.					
15. SUBJECT TERMS Lithium batteries; Storage batteries; Electric batteries; Electrochemical cells; Energy storage; Space missions; Spacecraft power supplies; Electric power supplies					
16. SECURITY CLASSIFICATION OF:			17. LIMITATION OF ABSTRACT  UU	18. NUMBER OF PAGES 18	19a. NAME OF RESPONSIBLE PERSON STI Help Desk (email: <a href="mailto:help@sti.nasa.gov">help@sti.nasa.gov</a> )
a. REPORT U	b. ABSTRACT U	c. THIS PAGE U			19b. TELEPHONE NUMBER (include area code) 443-757-5802





